

Article

Preparation of Chitosan-Based Hemostatic Sponges by Supercritical Fluid Technology

Hu-Fan Song¹, Ai-Zheng Chen^{1,2,3,*}, Shi-Bin Wang^{1,2,3}, Yong-Qiang Kang¹, Shi-Fu Ye¹, Yuan-Gang Liu^{1,2,3} and Wen-Guo Wu^{1,2,3}

- ¹ College of Chemical Engineering, Huaqiao University, Xiamen 361021, Fujian, China; E-Mails: hqushf@163.com (H.-F.S.); sbwang@hqu.edu.cn (S.-B.W.); hqukyq@126.com (Y.-Q.K.); yesu2008@126.com (S.-F.Y.); ygliu@hqu.edu.cn (Y.-G.L.); wuwenguo@hqu.edu.cn (W.-G.W.)
² Institute of Pharmaceutical Engineering, Huaqiao University, Xiamen 361021, Fujian, China;
³ Institute of Biomaterials and Tissue Engineering, Huaqiao University, Xiamen 361021, Fujian, China

* Author to whom correspondence should be addressed; E-Mail: azchen@hqu.edu.cn; Tel./Fax: +86-592-616-2326.

Received: 23 December 2013; in revised form: 7 March 2014 / Accepted: 20 March 2014 / Published: 27 March 2014

Abstract: Using ammonium bicarbonate (AB) particles as a porogen, chitosan (CS)-based hemostatic porous sponges were prepared in supercritical carbon dioxide due to its low viscosity, small surface tension, and good compatibility with organic solvent. Fourier transform infrared spectroscopy (FTIR) spectra demonstrated that the chemical compositions of CS and poly-(methyl vinyl ether-co-maleic anhydride) (PVM/MA) were not altered during the phase inversion process. The morphology and structure of the sponge after the supercritical fluid (SCF) process were observed by scanning electron microscopy (SEM). The resulting hemostatic sponges showed a relatively high porosity (about 80%) with a controllable pore size ranging from 0.1 to 200 μm . The concentration of PVM/MA had no significant influence on the porosity of the sponges. Comparative experiments on biological assessment and hemostatic effect between the resulting sponges and Avitene[®] were also carried out. With the incorporation of PVM/MA into the CS-based sponges, the water absorption rate of the sponges increased significantly, and the CS-PVM/MA sponges showed a similar water absorption rate (about 90%) to that of Avitene[®]. The results of the whole blood clotting experiment and animal experiment also demonstrated that the clotting ability of the CS-PVM/MA sponges was similar to that of Avitene[®]. All these results elementarily verified that the sponges prepared in this study were suitable for hemostasis and

demonstrated the feasibility of using SCF-assisted phase inversion technology to produce hemostatic porous sponges.

Keywords: chitosan; hemostatic sponge; porous structure; supercritical fluids

1. Introduction

Studies and applications of absorbable hemostatic material are meaningful to both hygiene and military [1]. Hemorrhage is one of the leading causes of death on the war field and in other contexts of trauma. This continuously stimulates the development of novel absorbable hemostatic materials [2]. Commonly used absorbable hemostatic materials include collagen and collagen fibers, fiber protein, oxidized cellulose and oxidized regenerated cellulose, medical hemostatic gelatin, alginate, and chitosan (CS) [3–6]. Among them, CS has been widely investigated because of its unique features. The CS-based hemostatic materials have been prepared in different forms which have been shown to possess no genetic toxicity, no subacute toxicity effects, no cytotoxicity, no hemolysis, good biological compatibility, and biodegradable properties [7,8]. For example, CS has been made into sponges to absorb a high amount of fluid (more than 20 times their dry weight) [9]; different molecular weight CS-based membranes have been developed for tissue regeneration and hemostasis [10]; the American company HemCon developed a hemostatic bandage whose main composition was chitosan and named it the HemCon Bandage; and the SAM (US) company extracted a mixture called Celox from shrimp shell and made it a hemostatic powder: one of its effective ingredients is chitosan [11]. However, the preparation methods in these studies mainly concentrated on particle leaching, electrospinning, gas foaming processes, and freeze drying technology [12–14]. The main disadvantages of these methods were the use of organic solvents and the special temperatures required. Since the presence of residual organic solvents is rigorously controlled by international safety regulations, a heavy downstream process is necessary to reduce the organic residue to a safe limit.

Over the past few decades, supercritical fluid (SCF) technology has been developed and widely utilized in tissue engineering and biomedical applications. It appears to be an interesting alternative to the traditional processing method [15,16]. Compared with the conventional methods mentioned above, the unique advantages of supercritical CO₂-based techniques include mild critical points ($T_c = 304.1$ K, $P_c = 7.38$ MPa), non-toxicity, non-flammability, the virtual absence of organic residue, and a relatively low price [17,18]. Recently, a process in which supercritical CO₂ replaces the liquid non-solvent for phase separation has been proposed. Our previous study [15] produced a porous nanostructured poly-L-lactide (PLLA) scaffold with interconnected pores by phase inversion, using supercritical CO₂ as an anti-solvent in the presence of ammonium bicarbonate (AB) particles. It confirmed the possibility of using supercritical fluid technology to produce porous material. The contact between the solvent and the supercritical CO₂ causes phase separation of the solution. The participation of supercritical fluid as the anti-solvent adds several advantages to the process. One of the most important advantages of using supercritical CO₂ is the fact that the final structure of the product can be tailored by simply tuning the operating parameters of pressure and temperature [19]. Additionally, when using CO₂ as an anti-solvent,

a subsequent drying step was avoided, and the porous structure obtained was a dry product free of residual solvent [20].

In this study, we attempted to prepare CS-based hemostatic porous sponges by phase inversion, using supercritical CO₂ as an anti-solvent in the presence of AB particles. We compared the prepared sponges with Avitene[®] in terms of morphology, porosity, water absorption rate, and clotting ability. A femoral artery hemorrhage mouse model was established to investigate the hemostatic effects.

2. Results and Discussion

2.1. The Morphology of the CS-Based Sponge

Figure 1 shows the schematic diagram of the apparatus for the SCF process and Figure 2 shows the optical images of the CS-based hemostatic sponges. The resulting shape can be controlled by changing the shape of the steel mold. It has been demonstrated that the morphology of the sponges could be reproduced accurately by the SCF phase inversion process [15]. In the phase inversion process, the properties of the final porous structure were mainly controlled by the precipitation temperature, the pressure of the bath, the flow rate of CO₂, the concentration of the casting solution, and the particle size of the porogen. Figure 3 shows the SEM images of the sponges. The results show that the pore size can vary from 0.1 to 200 μm because of the use of a porogen and the control of the supercritical fluid conditions. In tissue engineering, in order to properly identify an optimal pore size for maximal cell attachment, uniform scaffolds with a wider range of pore sizes were investigated. It was shown that different cell types would respond to different scaffold structures [21]. However, the hemostasis mechanism of CS has not been thoroughly understood until now. The hemostatic action of CS depends mainly on adhesion of red blood cells, aggregation of platelets for effective stimulation, activation of the complement system, and stimulation of other blood components to promote blood coagulation. Whether a wide range of pore size was good for hemostasis was not confirmed. However, the results of this study indicated that CS-based porous hemostatic sponges with a wide range of pore size can be prepared by SCF-assisted phase inversion, and this would be helpful for the further study of CS-based hemostatic materials.

Figure 1. Schematic diagram of the apparatus for the supercritical fluid (SCF) process.

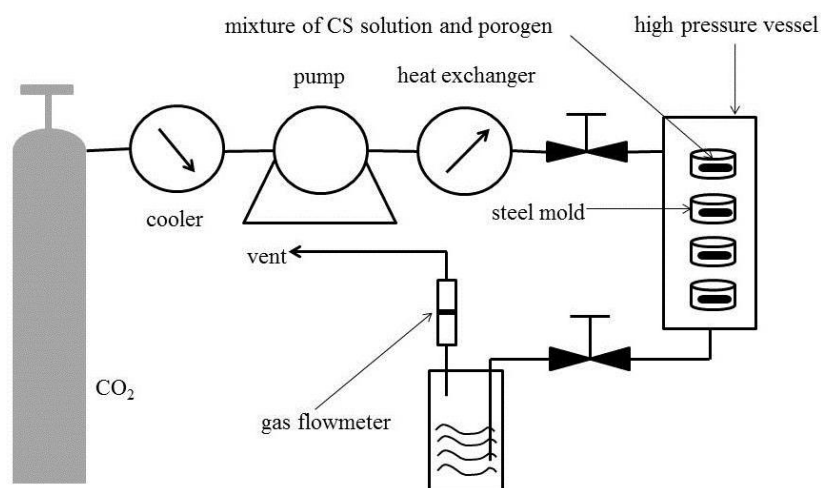


Figure 2. Optical digital photo of the porous sponge.

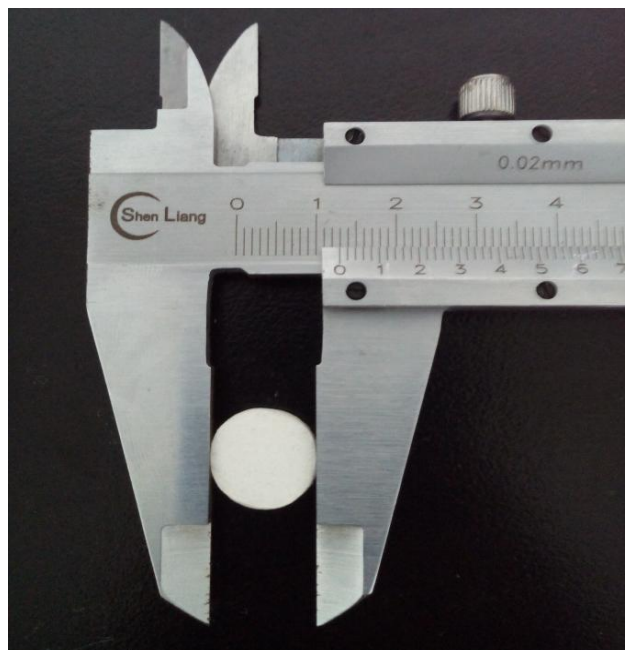
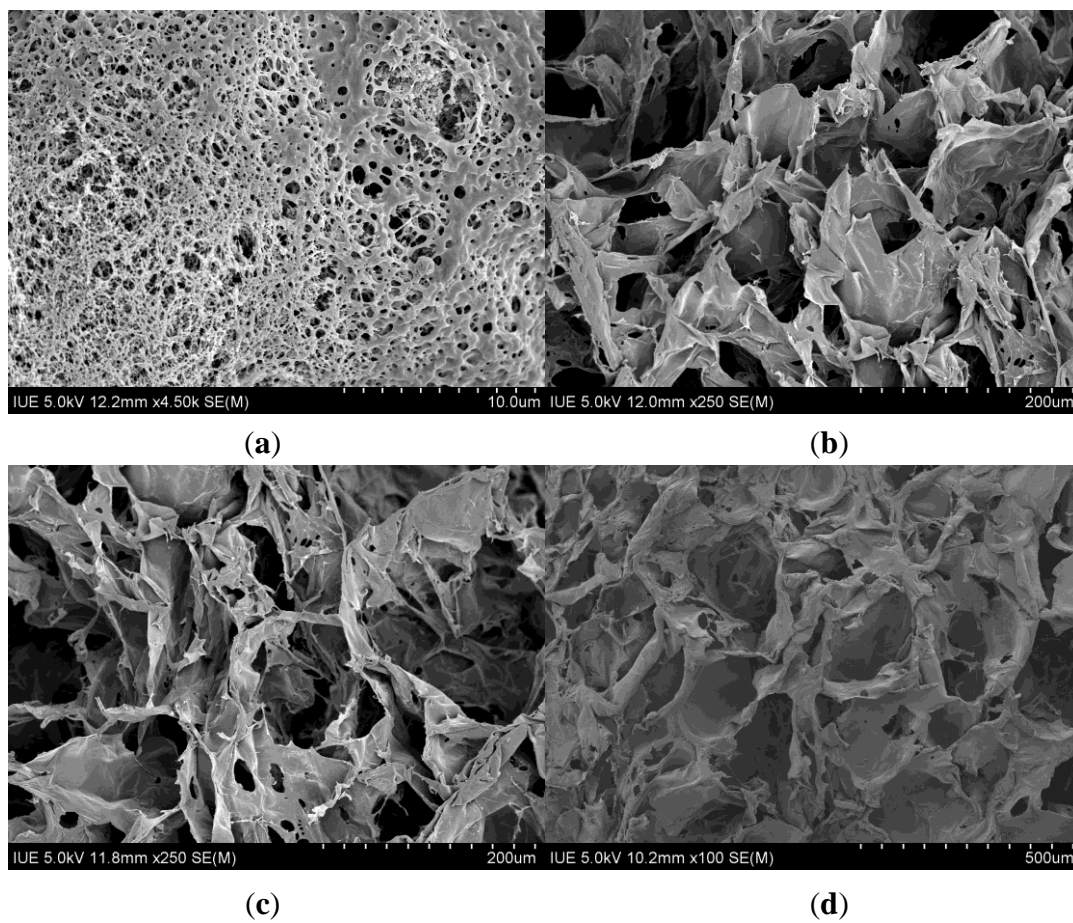


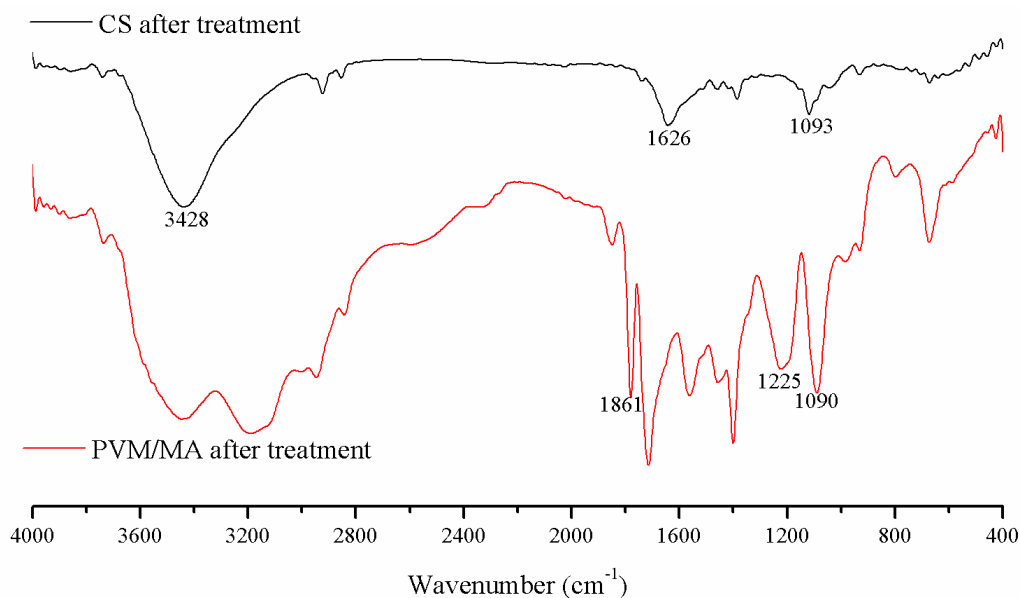
Figure 3. SEM photos of porous sponges with different mean pore sizes of (a) 0.1 μm ; (b) 60 μm ; (c) 80 μm ; and (d) 200 μm .



2.2. FTIR Spectra of CS and PVM/MA after Treatment

The FTIR spectra of the CS and PVM/MA after the SCF process are shown in Figure 4. In these spectra, the characteristic bands of chitosan and PVM/MA are indicated. For chitosan, the band at 3428 cm^{-1} was attributed to O–H and N–H stretching. The band at 1626 cm^{-1} was attributed to C=O stretching, and the band at 1093 cm^{-1} was attributed to C–O stretching. For PVM/MA, the bands at 1861 cm^{-1} , 1225 cm^{-1} , and 1090 cm^{-1} were attributed to C=O, C–O–C, and ether bonds, respectively. According to previous research [22,23] about the characteristic peaks of raw CS and PVM/MA, there were no changes in the chemical composition after the SCF process. The results indicate the same conclusion as in our previous study [15], that the supercritical process is a physical process and is capable of producing CS-based hemostatic materials.

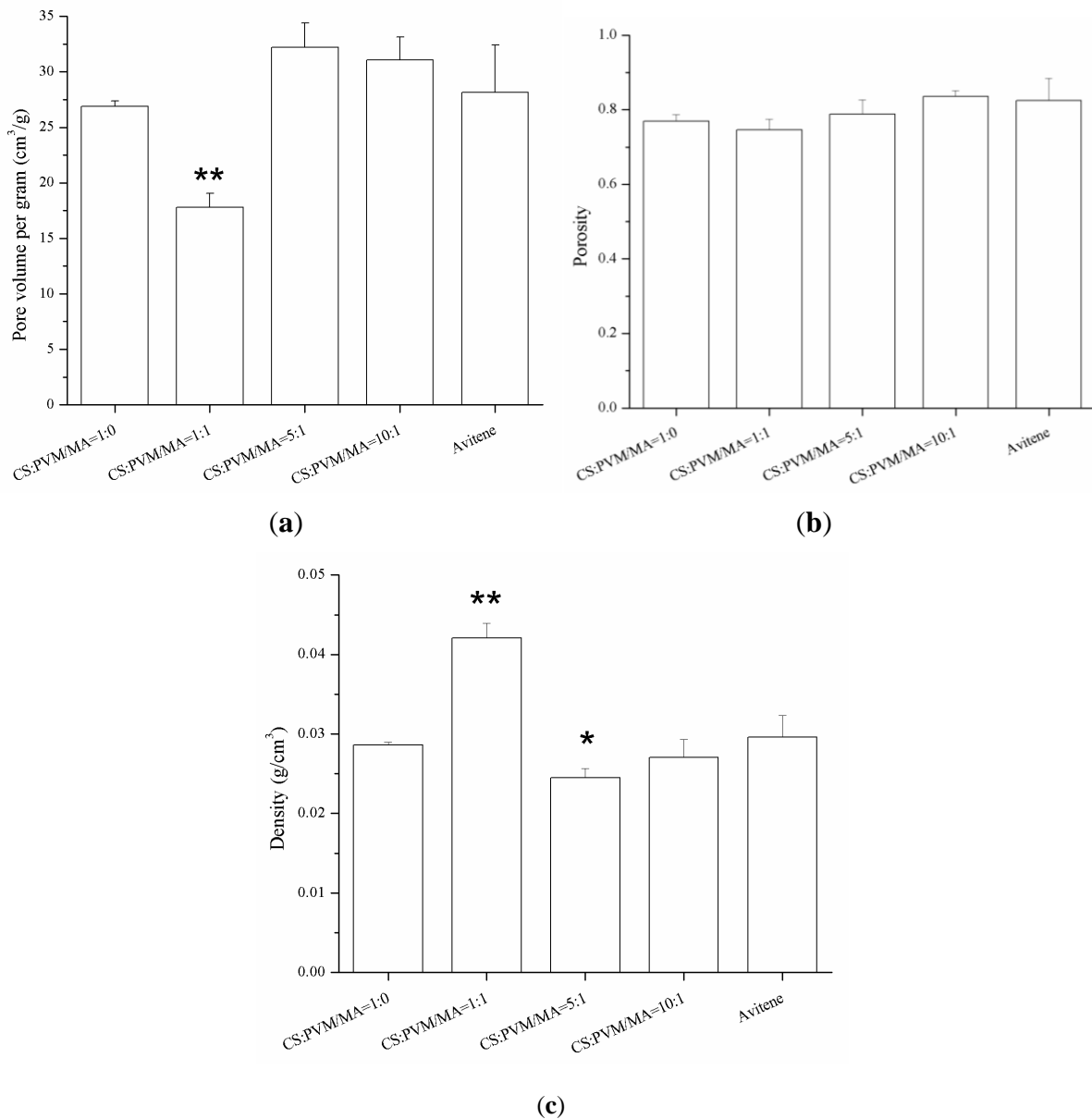
Figure 4. FTIR spectra of chitosan (CS) and poly-(methyl vinyl ether-co-maleic anhydride) (PVM/MA) after the SCF process.



2.3. Porosity of the Sponges

Some parameters related to the sponges, such as porosity, pore volume per gram, and density are exhibited in Figure 5. The porosities of the four kinds of sponges were all about 80%, which demonstrates that the PVM/MA had no significant influence on the porosity of the CS-based sponges. With the increase of PVM/MA, the density of the sponges increased and the pore volume per gram decreased greatly. The porogen has two functions. First, it mixed with polymer and solvent to form polymer/salt/solvent paste, thus the polymer/salt/solvent paste can be casted into the steel mold to form a designed shape. The second function of porogen is to increase the porosity of the hemostatic sponge. The experiment of producing samples without porogen was also carried out. However, the resulting sponge showed a lower porosity with a relatively high sclerosis and fragile structure. Thus, the sponge produced without using porogen is not suitable for hemostasis under this condition. In a word, porogen played an important role in this system.

Figure 5. (a) Pore volume per gram of plain CS, Avitene[®], and CS-PVM/MA sponges; (b) porosity of plain CS, Avitene[®], and CS-PVM/MA sponges; and (c) density of plain CS, Avitene[®], and CS-PVM/MA sponges. The “*” indicates a significant difference between the prepared sponge and Avitene when $p < 0.05$, while the “**” indicates a significant difference between the prepared sponge and Avitene when $p < 0.01$ (Student’s t-test, $n = 3$).

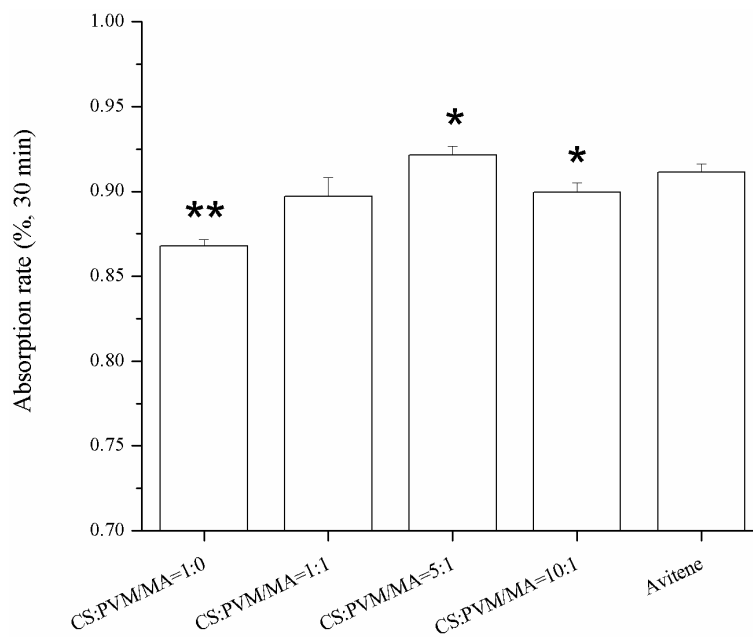


2.4. Water Absorption Rate

Sponges with a higher water absorption rate will absorb more blood at one time, which is important for an effective hemostasis. Figure 6 shows the water absorption rates of the different sponges in 30 min. The results show that the incorporation of the PVM/MA into the CS sponges improved the water absorption rate compared with the plain chitosan sponge. Previous studies [14,24] had reported that there were several parameters affecting the water absorption rate of sponges, including the hydrophilicity and the pore structure of the sponges. From the pore parameters of the sponges shown in Figure 5, it was found that the water absorption rate coincided well with the pore volume per gram. This

indicates that the pore volume per gram may be the dominant factor in the water absorption rate of the sponges with similar porosities. The high water absorption rate of the prepared CS-PVM/MA sponges was similar to that of Avitene®.

Figure 6. Water absorption rate of different sponges. The “*” indicates a significant difference between the prepared sponge and Avitene when $p < 0.05$, while the “**” indicates a significant difference between the prepared sponge and Avitene when $p < 0.01$ (Student’s t-test, $n = 3$).



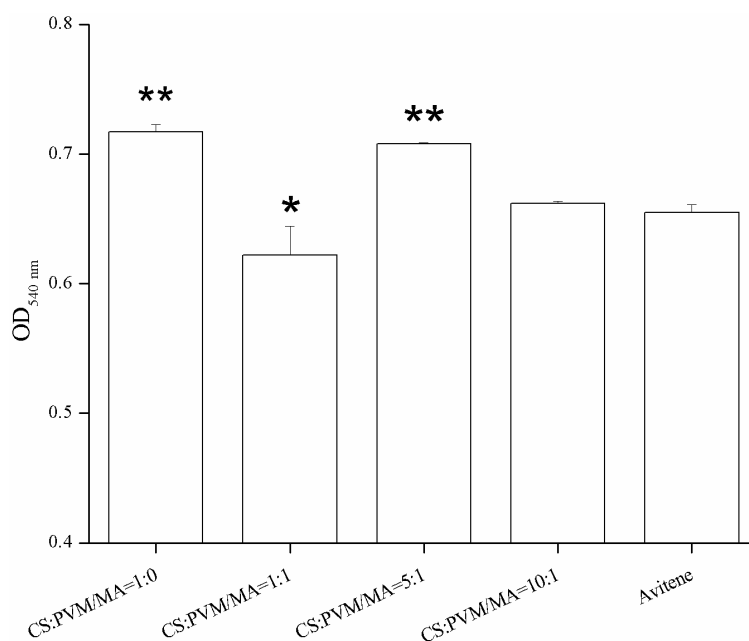
2.5. Results of Whole Blood Clotting Experiment

The whole blood clotting experiment was designed to test the *in vitro* clotting ability of the prepared sponge. The results of the whole blood clotting experiment are shown in Figure 7. A higher absorbance value meant a poorer clotting ability. Firstly, all of the CS-PVM/MA sponges had lower absorbance values than the plain CS sponge, which indicated that the clotting ability of the sponges was enhanced by the incorporation of PVM/MA. This was verified by Cochrum’s research [25], which indicated that the clotting ability of plain CS was not satisfactory compared with the other CS-based composites. PVM/MA is a polyanhydride and often used as a film forming agent, a denture adhesive, an adjuvant for transdermal patches in cosmetics and personal care products, and in the fabrication of drug-loaded polymer particles, due to its bioadhesive and mucoadhesive properties [22,26,27]. When PVM/MA is hydrolyzed, carboxylic groups are produced which enhance the ability of polymers to form hydrogen bonds with components from the mucosa [28]. The hydrogen bonds may also enhance the adsorption capacity of sponges for blood cells. Thus, the sponges incorporated with PVM/MA would possess a higher clotting ability.

When the water absorption rates were compared, it was noticeable that the CS-PVM/MA sponge (5:1, wt/wt) exhibited the highest water absorption rate but the lowest clotting ability, which indicated that the highest water absorption rate did not correspond to the highest clotting ability; some other characteristic, such as red blood cells adhesion, may be more decisive. However, it is generally accepted that the water

absorption rate is important to hemostasis in surgery. The use of sponges with a low water absorption rate may result in secondary hemorrhage or hemostatic failure.

Figure 7. Results of whole blood clotting experiment. The “*” indicates a significant difference between the prepared sponge and Avitene when $p < 0.05$, while the “**” indicates a significant difference between the prepared sponge and Avitene when $p < 0.01$ (Student’s t-test, $n = 3$).



2.6. Results of Animal Experiment

Figure 8 shows the photographic record of the femoral artery trauma model, and Figure 9 shows the results of the animal experiment, where a shorter hemostatic time indicated a higher *in vivo* clotting ability of the sponge. In each case, the bleeding stopped within 70 s. From the statistical analysis, the composition CS:PVM/MA 1:1 shows a significant difference with Avitene except for water absorption rate, porosity and hemostatic time. It possesses a better clotting ability than other compositions and Avitene in the whole blood experiments. Compared with Avitene, the composition 1:0 (plain chitosan) shows a significantly worse clotting ability in the whole blood experiment and animal experiment while the other two compositions share similar parameters and clotting ability. Thus, we can conclude that the prepared sponge was enhanced with the incorporation of PVM/MA into the CS-based sponges. Among them, the hemostatic ability of composition CS:PVM/MA 1:1 is significantly improved and similar to Avitene *in vivo* and *in vitro*. It was also observed during the treatment that the adsorption rate and adhesion of the CS-PVM/MA sponge were better than those of the plain chitosan sponge; when the blood flowed briskly, blood was seen to leak from the pore structure of the plain CS sponge, while this phenomenon was absent when using the CS-PVM/MA sponges. This may be because the poor flexibility of the CS sponges results in crushing of the inner pore structure when the sponge is compressed during use, while the incorporation of PVM/MA makes the sponges more flexible and adhesive, thus increasing their hemostatic effect.

Our previous study [29] has verified that the HFIP residual in the samples produced by SCF-assisted phase technology was controlled as low as 20 ppm. Chitosan has been widely used in tissue engineering and introduced as cell-carrier material and discussed in terms of the biocompatibility with chondrocytes. Results indicated that chitosan was suitable as a carrier-material for the transplant of chondrocytes [30]. It is also proved that PVM/MA was not only safe as cosmetic ingredients but also suitable for other use and would not raise any significant toxicity [31]. We believe that the low organic solvent residue (as low as 20 ppm) of the samples prepared by supercritical process will not cause an additional toxicity to the materials (CS/PVMMMA) which have been proved as biocompatible and nontoxic materials. However, the detailed biological evaluation includes the cytotoxicity measurements should be carried out to confirm this conclusion.

Figure 8. Photographs of (a) mouse leg after removing the hair; (b) trauma model on femoral artery of mouse; and (c) the hemostatic effect of sponge on mouse.

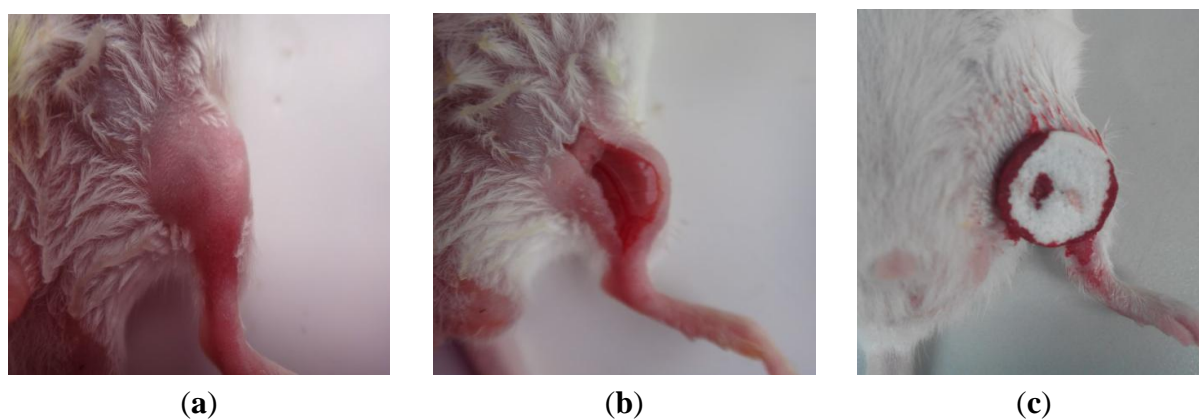
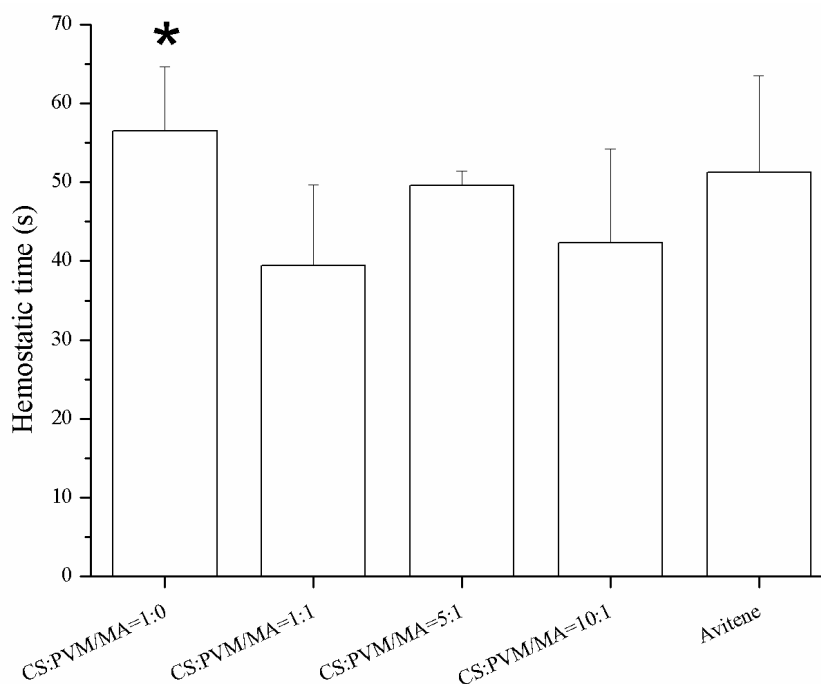


Figure 9. Hemostasis time of different sponges on mouse femoral artery. The “*” indicates a significant difference between the prepared sponge and Avitene ($p < 0.05$, Student’s t-test, $n = 12$).



3. Experimental Section

3.1. Materials

3.1.1. Experimental Animals

Kung Ming mice were provided by the Fuzhou Experimental Company (Fuzhou, China). They had free access to water and food, and were used for experiments after 7 days.

3.1.2. Other Main Materials

CS with a low viscosity was purchased from the Aladdin Co. (Los Angeles, CA, USA). AB (99.8% purity) was purchased from the Sinopharm Chemical Reagent Co., Ltd. (Shanghai, China), and CO₂ of 99.9% purity was purchased from the Rihong Air Products Co., Ltd. (Xiamen, China). PVM/MA (analytical purity) was purchased from Sigma-Aldrich (St. Louis, MO, USA). Hexafluoroisopropanol (HFIP, analytical purity) was purchased from Sigma-Aldrich (USA).

3.2. Preparation of Hemostatic Sponges

CS solution was prepared by dissolving CS in HFIP [19]; the solution was stirred for 6 h until it became homogeneous. AB particles (300–600 μm) were added into the solution which was then mixed vigorously. The polymer/salt/solvent paste was cast into the steel mold, and then the resulting samples with a diameter of 1.0 cm and height of 5.0 mm were placed in the high-pressure vessel. Supercritical CO₂ was pumped into the high-pressure vessel to achieve the desired pressure (15 MPa) and temperature (308 K). After treatment for 1.5 h, the vessel was flushed with fresh CO₂ at a constant flow rate (approximately 5 g min⁻¹) for 1.5 h to remove the organic solvent. The temperature in the high pressure vessel was increased to 313 K to confirm the decomposition of the AB particles. During this process, the pressure and temperature were kept constant. The system was then rapidly depressurized to atmospheric pressure within 2 min.

The preparation process of the CS-PVM/MA hemostatic sponges was similar to that of the CS sponges. After the CS was dissolved in HFIP, the PVM/MA solution in acetone was added into the chitosan solution with vigorous stirring, and the subsequent steps were the same as in the preparation of the CS sponges. In this study, CS-PVM/MA sponges with different compositions (1:1, 5:1, and 10:1, wt/wt) were prepared.

3.3. Surface Morphology Observation

CS-based hemostatic sponges were fractured in liquid nitrogen. Samples were sputter coated with gold for 180 s (Ion Sputter E-1010, Hitch, Japan). The overall sponge surface morphology was analyzed using SEM equipment (S-4800, Hitch, Japan).

3.4. FTIR Analysis

Samples of approximately 1 mg in weight were pressed into a pellet with 200 mg of potassium bromide, and FTIR spectra were collected in continuous scan mode (wavenumber range: 4000–400 cm^{-1}) and at a resolution of 10 cm^{-1} on a Nicolet iS10 system (Thermo, Waltham, MA, USA).

3.5. Porosity of Sponges

The porosity and other pore parameters of the sponges were determined according to the method described in the reference [32]. Firstly, the pycnometer was filled with anhydrous ethanol, and the total weight was recorded as W_1 ; the sample was weighed (W_s) and then put into the pycnometer. After ultrasonic degassing, the pycnometer was filled with ethanol again and weighed (W_2). The sample was then taken out, and the weight of the remaining ethanol together with the pycnometer was recorded as W_3 ; ρ was the density of the ethanol under the experimental conditions. The pore parameters of the sponges can be calculated as follows:

$$\varepsilon = (W_2 - W_3 - W_s) / (W_2 - W_3) \quad (1)$$

$$\rho_s = \rho W_s / (W_1 - W_3) \quad (2)$$

$$\pi = (W_2 - W_3 - W_s) / \rho W_s \quad (3)$$

where ρ , ε , ρ_s , and π represent the density of ethanol, porosity, sponge density, and pore volume per gram, respectively.

3.6. Water Absorption Rate

(1) Five hundred milliliters of a simulation solution was prepared (containing 4.199 g of sodium chloride and 0.139 g of anhydrous calcium chloride), which had an ion content equal to that of human serum or percolate on the surface of a wound.

(2) The samples (0.5 cm \times 0.5 cm, the weight was recorded as m_1) were put into a drying oven (80 $^\circ\text{C}$), weighed every 5 min until the variation was less than 0.0005 g, and then placed in a petri dish.

(3) A certain amount of simulation solution (40 times heavier than the sample) was added to the petri dish (preheated to 37 ± 1 $^\circ\text{C}$).

(4) All the petri dishes were placed in a drying oven and kept for 30 min at $37(\pm 1)$ $^\circ\text{C}$. One end of the samples was clamped with tweezers for 30 s to remove the water on the sample's surface, and then the weight was recorded as m_2 .

$$\text{Water absorption rate} = \frac{m_2 - m_1}{m_2} \times 100\% \quad (4)$$

3.7. The Whole Blood Clotting Experiment

The sponges were cut into 0.5 cm \times 0.5 cm squares and placed into tubes. Then, 0.2 mL of rabbit whole blood (using sodium citrate as an anticoagulant) and 20 μL of CaCl_2 solution (0.2 M) were dispensed onto the surface of the sponges. The tubes were incubated at 37 $^\circ\text{C}$ and 30 rpm for 10 min.

Next, 25 mL of distilled water was added to the tubes slowly. The unclotted blood cells were dissolved with distilled water and measured at 540 nm (UV-VIS). The absorbance of 0.2 mL of rabbit whole blood in 25 mL of distilled water was used as a negative control.

3.8. The Femoral Artery Hemorrhage Mouse Model

Kung Ming mice were chosen to investigate the hemostatic effects. Each group comprised 10 mice. The Kung Ming mice whose weight was about 20–30 g were picked out as experimental animals after being raised under experimental conditions for one week. The mice were given intraperitoneal anesthesia with 2% pento-barbital sodium, and the hair on one leg of each mouse was removed with 8% Na₂S depilatory solution. The femoral artery was cut with a sterilized bistoury, resulting in an open wound of 0.5 cm, and the time was recorded immediately. After free bleeding for 10 s, a square of hemostatic sponge (50 mm²) was used to cover the wound. The hemostasis time was recorded when the wound stopped bleeding. The experiments were carried out in accordance with the guidelines issued by the Ethical Committee of Huaqiao University.

3.9. Statistical Analysis

All quantitative data were expressed as means \pm standard deviations. Differences between means were analyzed for statistical significance using the Student's t-test. p-values less than 0.05 were considered statistically significant.

4. Conclusions

CS-based hemostatic sponges with a porous structure were successfully prepared using AB particles as a porogen in a supercritical CO₂ process. The sponges possessed the structural characteristics of large pores and micro pores which varied from 0.1 to 200 μ m in diameter, and they can be utilized for different needs. They were characterized by a high porosity (about 80%) and a porous structure that allows red blood cells to form erythrocyte clots or plugs. The incorporation of PVM/MA did not alter the sponges' porosities significantly, but the water absorption rate and the *in vivo* and *in vitro* clotting ability of the sponges were improved. The porosity may be determined by the dosage of the porogen and the parameters of the SCF process. The results of the whole blood experiment and the animal experiment also indicate that the prepared CS-PVM/MA sponges showed a similar clotting ability to that of Avitene[®]. This confirmed the feasibility of using SCF technology to produce hemostatic sponges.

Acknowledgments

Financial supports from Natural Science Foundation of China (51103049 and 31170939), Promotion Program for Young and Middle-aged Teacher in Science and Technology Research of Huaqiao University (ZQN-PY107), Science and Technology Project of Fujian Province (2013Y2002) and Specialized Research Fund for the Doctoral Program of Higher Education (20133501110003) are gratefully acknowledged.

Author Contributions

Hu-Fan Song contributed to supercritical experiments and preparation of the manuscript, Ai-Zheng Chen and Shi-Bin Wang designed the project and revised the manuscript, Yong-Qiang Kang and Shi-Fu Ye were involved in animal experiments, Yuan-Gang Liu and Wen-Guo Wu contributed to characterization of the sponges.

Conflicts of Interest

The authors declare no conflict of interest.

References

1. Gu, R.L.; Sun, W.Z.; Zhou, H.; Wu, Z.; Meng, Z.Y.; Zhu, X.X.; Tang, Q.; Dong, J.; Dou, G.F. The performance of a fly-larva shell-derived chitosan sponge as an absorbable surgical hemostatic agent. *Biomaterials* **2010**, *31*, 1270–1277.
2. Janvikul, W.; Uppanan, P.; Thavornytikarn, B.; Krewraing, J.; Prateepasen, R. *In vitro* comparative hemostatic studies of chitin, chitosan, and their derivatives. *J. Appl. Polym. Sci.* **2006**, *102*, 445–451.
3. Igai, H.; Yamamoto, Y.; Chang, S.S.; Yamamoto, M.; Tabata, Y.; Yokomise, H. Tracheal cartilage regeneration by slow release of basic fibroblast growth factor from a gelatin sponge. *J. Thorac. Cardiovasc. Surg.* **2007**, *134*, 170–175.
4. Schonauer, C.; Tessitore, E.; Barbagallo, G.; Albanese, V.; Moraci, A. The use of local agents: Bone wax, gelatin, collagen, oxidized cellulose. *Eur. Spine J.* **2004**, *13*, S89–S96.
5. Björnses, K.; Holst, J. Various local hemostatic agents with different modes of action; an *in vivo* comparative randomized vascular surgical experimental study. *Eur. J. Vasc. Endovasc. Surg.* **2007**, *33*, 363–370.
6. Boateng, J.S.; Matthews, K.H.; Stevens, H.N.E.; Eccleston, G.M. Wound healing dressings and drug delivery systems: A review. *J. Pharm. Sci.* **2008**, *97*, 2892–2923.
7. Anaya, P.; Cárdenas, G.; Lavayen, V.; Garc á, A.; O'Dwyer, C. Chitosan gel film bandages: Correlating structure, composition, and antimicrobial properties. *J. Appl. Polym. Sci.* **2013**, *128*, 3939–3948.
8. Zhang, J.L.; Xia, W.S.; Liu, P.; Cheng, Q.Y.; Tahi, T.; Gu, W.X.; Li, B. Chitosan modification and pharmaceutical/biomedical applications. *Mar. Drugs* **2010**, *8*, 1962–1987.
9. Jayakumar, R.; Prabakaran, M.; Sudheesh Kumar, P.T.; Nair, S.V.; Tamura, H. Biomaterials based on chitin and chitosan in wound dressing applications. *Biotechnol. Adv.* **2011**, *29*, 322–337.
10. Freitas, R.; Spin-Neto, R.; Spolidório, L.C.; Campana-Filho, S.P.; Marcantonio, R.A.C.; Marcantonio, E., Jr. Different molecular weight chitosan-based membranes for tissue regeneration. *Materials* **2011**, *4*, 380–389.
11. Millner, R.W.J.; Lockhart, A.S.; Bird, H.; Alexiou, C. A new hemostatic agent: initial life-saving experience with Celox (chitosan) in cardiothoracic surgery. *Ann. Thorac. Surg.* **2009**, *87*, e13–e14.

12. Nwe, N.; Furuike, T.; Tamura, H. The mechanical and biological properties of chitosan scaffolds for tissue regeneration templates are significantly enhanced by chitosan from *Gongronella butleri*. *Materials* **2009**, *2*, 374–398.
13. Feng, C.; Khulbe, K.C.; Matsuura, T. Recent progress in the preparation, characterization, and applications of nanofibers and nanofiber membranes via electrospinning/interfacial polymerization. *J. Appl. Polym. Sci.* **2010**, *115*, 756–776.
14. Jiao, Y.; Liu, Z.; Zhou, C. Fabrication and characterization of PLLA-chitosan hybrid scaffolds with improved cell compatibility. *J. Biomed. Mater. Res. Part A* **2007**, *80*, 820–825.
15. Deng, A.H.; Chen, A.Z.; Wang, S.B.; Li, Y.; Liu, Y.G.; Cheng, X.X.; Zhao, Z.; Lin, D.L. Porous nanostructured poly-L-lactide scaffolds prepared by phase inversion using supercritical CO₂ as a nonsolvent in the presence of ammonium bicarbonate particles. *J. Supercrit. Fluids* **2013**, *77*, 110–116.
16. Reverchon, E.; Cardea, S. Supercritical fluids in 3-D tissue engineering. *J. Supercrit. Fluids* **2012**, *69*, 97–107.
17. Chen, A.Z.; Li, L.; Wang, S.B.; Zhao, C.; Liu, Y.G.; Wang, G.Y.; Zhao, Z. Nanonization of methotrexate by solution-enhanced dispersion by supercritical CO₂. *J. Supercrit. Fluids* **2012**, *67*, 7–13.
18. Reverchon, E.; Cardea, S.; Rappo, E.S. Membranes formation of a hydrosoluble biopolymer (PVA) using a supercritical CO₂-expanded liquid. *J. Supercrit. Fluids* **2008**, *45*, 356–364.
19. Duarte, A.R.C.; Mano, J.F.; Reis, R.L. The role of organic solvent on the preparation of chitosan scaffolds by supercritical assisted phase inversion. *J. Supercrit. Fluids* **2012**, *72*, 326–332.
20. Matsuyama, H.; Yamamoto, A.; Yano, H.; Maki, T.; Teramoto, M.; Mishima, K.; Matsuyama, K. Effect of organic solvents on membrane formation by phase separation with supercritical CO₂. *J. Membr. Sci.* **2002**, *204*, 81–87.
21. O'Brien, F.J.; Harley, B.A.; Yannas, I.V.; Gibson, L.J. The effect of pore size on cell adhesion in collagen-GAG scaffolds. *Biomaterials* **2005**, *26*, 433–441.
22. Chen, A.Z.; Wang, G.Y.; Wang, S.B.; Feng, J.G.; Liu, Y.G.; Kang, Y.Q. Preparation of poly-(methyl vinyl ether-co-maleic anhydride) nanoparticles by solution-enhanced dispersion by supercritical CO₂. *Materials* **2012**, *5*, 1841–1852.
23. Kang, Y.; Yang, C.; Ouyang, P.; Yin, G.; Huang, Z.; Yao, Y.; Liao, X. The preparation of BSA-PLLA microparticles in a batch supercritical anti-solvent process. *Carbohydr. Polym.* **2009**, *77*, 244–249.
24. Kang, P.L.; Chang, S.J.; Manousakas, I.; Lee, C.W.; Yao, C.H.; Lin, F.H.; Kuo, S.M. Development and assessment of hemostasis chitosan dressings. *Carbohydr. Polym.* **2011**, *85*, 565–570.
25. Chiu, M.M.C.; Cochrum, K.C.; Parker, H.R. Fibrinogen/Chitosan Hemostatic Agents. U.S. Patent 5773033, 30 June 1998.
26. Elizondo, E.; Córdoba, A.; Sala, S.; Ventosa, N.; Veciana, J. Preparation of biodegradable poly (methyl vinyl ether-co-maleic anhydride) nanostructured microparticles by precipitation with a compressed antisolvent. *J. Supercrit. Fluids* **2010**, *53*, 108–114.
27. Yoncheva, K.; Lizarraga, E.; Irache, J.M. Pegylated nanoparticles based on poly(methyl vinyl ether-co-maleic anhydride): Preparation and evaluation of their bioadhesive properties. *Eur. J. Pharm. Sci.* **2005**, *24*, 411–419.

28. Cerchiara, T.; Luppi, B.; Chidichimo, G.; Bigucci, F.; Zecchi, V. Chitosan and poly(methyl vinyl ether-co-maleic anhydride) microparticles as nasal sustained delivery systems. *Eur. J. Pharm. Biopharm.* **2005**, *61*, 195–200.
29. Deng, A.H. Fabrication of the SF/PLLA Compound Tissue Engineering Scaffolds by Supercritical Fluids Technology. Ph.D. Thesis, Huaqiao University, Xiamen, China, May 2013.
30. Suh, J.K.F.; Matthew, H.W.T. Application of chitosan-based polysaccharide biomaterials in cartilage tissue engineering: A review. *Biomaterials* **2000**, *21*, 2589–2598.
31. Burnett, C.L.; Bergfeld, W.F.; Belsito, D.V.; Hill, R.A.; Klaassen, C.D.; Liebler, D.C.; Marks, J.G., Jr.; Shank, R.C.; Slaga, T.J.; Snyder, P.W.; *et al.* Final report of the amended safety assessment of PVM/MA copolymer and its related salts and esters as used in cosmetics. *Int. J. Toxicol.* **2011**, *30*, 128S–144S.
32. Huang, W.; Shi, X.T.; Ren, L.; Du, C.; Wang, Y.J. PHBV microspheres—PLGA matrix composite scaffold for bone tissue engineering. *Biomaterials* **2010**, *31*, 4278–4285.

© 2014 by the authors; licensee MDPI, Basel, Switzerland. This article is an open access article distributed under the terms and conditions of the Creative Commons Attribution license (<http://creativecommons.org/licenses/by/3.0/>).